Since January 2020 Elsevier has created a COVID-19 resource centre with free information in English and Mandarin on the novel coronavirus COVID-19. The COVID-19 resource centre is hosted on Elsevier Connect, the company's public news and information website.

Molecular Immunology 47 (2010) 2575–2586

Contents lists available at ScienceDirect

Molecular Immunology

journal homepage: www.elsevier.com/locate/molimm

SARS spike protein induces phenotypic conversion of human B cells to macrophage-like cells

Shu-Fen Chiang[a,1], Tze-Yi Lin[b,1], Kuan-Chih Chow[c,*], Shiow-Her Chiou[a,*]

[a] Graduate Institute of Microbiology and Public Health, National Chung Hsing University, 250 Kuo Kuang Road, Taichung 40227, Taiwan
[b] Department of Pathology, College of Medicine, China Medical University and China Medical University Hospital, Taichung, Taiwan
[c] Graduate Institute of Biomedical Sciences, National Chung Hsing University, Taichung, Taiwan

ARTICLE INFO

Article history:
Received 18 October 2009
Received in revised form 28 June 2010
Accepted 29 June 2010
Available online 27 July 2010

Keywords:
SARS-associated coronavirus
B cell
Macrophage
Mac-1 (CD11b)
Hypoxia

ABSTRACT

Massive aggregations of macrophages are frequently detected in afflicted lungs of patients with severe acute respiratory syndrome-associated coronavirus (SARS-CoV) infection. In vitro, ectopic expression of transcription factors, in particular CCAAT/enhancer-binding protein alpha (C/EBPα) and C/EBPβ, can convert B cells into functional macrophages. However, little is known about the specific ligands responsible for such phenotype conversion. Here, we investigated whether spike protein of SARS-CoV can act as a ligand to trigger the conversion of B cells to macrophages. We transduced SARS-CoV spike protein-displayed recombinant baculovirus (SSDRB), vAtEpGS688, into peripheral B cells and B lymphoma cells. Cell surface expression of CD19 or Mac-1 (CD11b) was determined by flow cytometry. SSDRB-mediated changes in gene expression profiles of B lymphoma cells were analyzed by microarray. In this report, we showed that spike protein of SARS virus could induce phenotypic conversion of human B cells, either from peripheral blood or B lymphoma cells, to macrophage-like cells that were steadily losing the B-cell marker CD19 and in turn expressing the macrophage-specific marker Mac-1. Furthermore, we found that SSDRB enhanced the expression of CD86, hypoxia-inducible factor-1α (HIF1α), suppressor of cytokine signaling (SOCS or STAT-induced STAT inhibitor)-3, C/EBPβ, insulin-like growth factor-binding protein 3 (IGFBP3), Krüpple-like factor (KLF)-5, and CD54, without marked influence on C/EBPα or PU.1 expression in transduced cells. Prolonged exposure to hypoxia could also induce macrophage-like conversion of B cells. These macrophage-like cells were defective in phagocytosis of red fluorescent beads. In conclusion, our results suggest that conversion of B cells to macrophage-like cells, similar to a pathophysiological response, could be mediated by a devastating viral ligand, in particular spike protein of SARS virus, or in combination with severe local hypoxia, which is a condition often observed in afflicted lungs of SARS patients.

1. Introduction

Massive aggregations of macrophages are frequently detected in afflicted lungs of patients with severe acute respiratory syndrome-associated coronavirus (SARS-CoV) infection (Chow et al., 2004). Such a phenomenon had been suggested to be caused by infection-induced expression of IL-8 in the infected sites (Chang et al., 2004). However, available *in vitro* data do not fully interpret the pathological findings in which only macrophages were profusely detected in the afflicted lung. No evident neutrophil or lymphocyte infiltration is found in the traumatized area, which is unusual for general virus infection (Chow et al., 2004). Moreover, the estimated volume of atypical macrophages (Chow et al., 2004), which are distinct from alveolar macrophages, is well beyond the number of monocytes that can be provided by a patient's bone marrow within such a short time of virus infection. These clinical data suggest that other sources might be responsible for the unusual presence of macrophages. Based on the atrophic white pulp of spleen and the absence of lymphocytes in the damaged lung, it was proposed that SARS virus infection-specific product(s) could be potentially lymphotoxic (Chow et al., 2004; Nicholls et al., 2003; Zhan et al., 2006). The lack of evident karyorrhexis (Chiu et al., 2000) within the afflicted lung, however, argued against lymphotoxicity of SARS-CoV infection. These data prompt us to speculate that certain component(s) of SARS-CoV or microenvironmental conditions of SARS-CoV infection could act as the ligand or inducing factor for the conversion of lymphocytes to macrophages.

Traditionally, different blood cell types are all derived from a common hematopoietic stem cell, and the differentiation is considered irreversible; that is, following the commitment of

* Corresponding authors. Tel.: +886 4 2285 1343; fax: +886 4 2285 9270.
E-mail addresses: kcchow@dragon.nchu.edu.tw (K.-C. Chow), shchiou@dragon.nchu.edu.tw (S.-H. Chiou).
[1] The first two authors contributed equally to this work.

0161-5890/$ – see front matter © 2010 Elsevier Ltd. All rights reserved.
doi:10.1016/j.molimm.2010.06.014

multipotent progenitors, differentiation of hematopoietic cells becomes lineage-restricted (Akashi et al., 2000; Alexander, 1998; Heyworth et al., 2002; Stanley and Jubinsky, 1984). This irreversible process is normally directed by a series of specific growth factors, cytokines, and the expression of corresponding receptors (Akashi et al., 2000; Alexander, 1998; Stanley and Jubinsky, 1984). Interestingly, by examining the gene expression profile of hematopoiesis, several studies have found that transcription factors, such as AML-1, CCAAT/enhancer-binding protein alpha (C/EBPα), C/EBPβ, C/EBPε, E2A, GATA-1, GATA-2, c-myb, PU.1, and retinoic acid receptor (RAR, RXR), are essential for normal blood formation (Heyworth et al., 2002; Nakajima et al., 1994; Reddy et al., 2002; Xie et al., 2004). A deficiency in one of these factors impedes hematopoiesis and produces a variety of intermediate precursors of blood cells (Laslo et al., 2006; Loose and Patient, 2006; Wang et al., 2006). Replenishment of the specific factors, either alone or in combination, reestablishes hematopoiesis in gene-deficient cells or in differentiation-interrupted precursors of the same lineage. Enforced expression of those factors in progenitors of different lineages, however, prevents these cells from differentiating into the predetermined progeny cell types. Instead, these cells differentiate into transcription factor-specified lineages (Reddy et al., 2002; Wang et al., 2006; Xie et al., 2004). An elegant study by Xie et al. (2004) showed that ectopic expression of C/EBPα and C/EBPβ in mature B cells led to the inhibition of B-cell-specific activator protein (BSAP, also called Pax5) and the downregulation of its target CD19. Moreover, C/EBPα and C/EBPβ acted in synergy with endogenous PU.1 to remodel the transcription network and upregulate the expression of the myeloid marker Mac-1 (Xie et al., 2004). Others reported that C/EBPα could direct differentiation of hematopoietic progenitor cells into granulocytes (including neutrophils) while the enforced expression of PU.1 could promote differentiation into monocytes (Reddy et al., 2002; Wang et al., 2006). Coexpression of both C/EBPα and PU.1, however, prompts cells to express both markers of neutrophils and monocytes (Laslo et al., 2006). These observations suggest that a reprogrammed "transcription network" can direct progenitor blood cells onto different differentiation paths. However, the specific ligands, such as cytokines, growth factors, or other extracellular signals, responsible for such phenotype conversion are mostly unknown.

In this study, we investigated whether spike protein of SARS-CoV can act as a ligand to trigger the conversion of B cells to macrophages. Moreover, because SARS infection might provoke severe local hypoxia in the afflicted lung, we also examined the effect of hypoxia on the phenotypic conversion of B cells.

Our results show that spike protein of SARS displayed on recombinant baculovirus or prolonged exposure to hypoxia can trigger the conversion of peripheral B cells and B lymphoma cells into Mac-1 positive macrophage-like cells.

2. Materials

2.1. Cell lines and blood samples

CA46, HT, Toledo, LADC, H226, A549, and H125 cell lines were obtained from ATCC (Manassas, VA, USA). Cells were maintained in RPMI 1640 supplemented with 10% fetal calf serum, 100 I.U./mL penicillin and 100 μg/mL streptomycin (Hyclone, Logan, UT, USA) in a humidified incubator at 37 °C with 5% CO_2.

2.2. Isolation of mouse alveolar type II pneumocytes (ATII cells) and preparation of peripheral B lymphocytes

Eight-week-old male BALB/c mice were obtained from the National Animal Center (Taipei, Taiwan). Mouse ATII cells were isolated from freshly dissected lungs and characterized by using a previously described method with some modifications (Corti et al., 1996). The purity of the isolated ATII cells was determined by their morphology and immunocytochemistry to surfactant protein B (Chemicon, Temecula, CA).

Peripheral white blood cells (WBCs) were isolated from healthy donors through Histopaque (Sigma, St. Louis, MO, USA) density gradient centrifugation. B lymphocytes were purified by anti-CD19-conjugated magnet dynabeads (Dynabeads® CD19 Pan B, Invitrogen Taiwan, Ltd., Taipei, Taiwan). Viable B cells were harvested from the beads by using DETACHaBEAD® CD19 (Invitrogen Taiwan, Ltd., Taipei, Taiwan). Briefly, peripheral WBCs were suspended in phosphate-buffered saline (PBS) with 0.1% bovine serum albumin (BSA) and then incubated with anti-CD19-conjugated magnet dynabeads at 4 °C for 20 min. The reaction mixture was then placed on a magnet to attract cells that expressed CD19 on their membrane. Magnet-bound cells were washed 4 times with PBS and then detached from the beads by DETACHaBEAD® CD19. The purity of the isolated cells was determined by immunocytochemistry to anti-CD19. These $CD19^+$ B cells were cultured in RPMI 1640 supplemented with 10% fetal calf serum, 100 I.U./mL penicillin, and 100 μg/mL streptomycin in a humidified incubator at 37 °C with 5% CO_2.

2.3. Recombinant baculovirus, transduction, and electroporation

Recombinant baculovirus vAtEpGS688 expressing amino acids 17–688 of SARS-CoV spike protein on the surface of its envelope (Chang et al., 2004) and vAtE vector control were kindly provided by Dr. Y.-C. Chao (Institute of Molecular Biology, Academia Sinica, Nankang, Taipei, Taiwan). These vAtE-derived recombinant baculoviruses carry an *EGFP* gene in the viral genome, which is under the control of the CMV promoter. If such recombinant viruses can be transduced into mammalian cells, their viral genome can express EGFP for fluorescence detection (Chang et al., 2004). The vAtE control vector is identical to vAtEpGS688 except that it does not express SARS-CoV spike protein. Recombinant baculovirus vAtEpGS688 has been demonstrated to be able to enter human lung cells and induce chemokine with high efficiency (Chang et al., 2004).

The virus was amplified with multiplicity of infection (MOI) of 0.1 for 4 days in *Spodoptera frugiperda* (Sf21) cells (Clontech, Mountain View, CA, USA), and then harvested from the culture medium by centrifugation at $800 \times g$ for 5 min to remove cell debris. Viral titer was measured by real-time polymerase chain reaction. The transduction reactivity of the virus was determined on Vero E6 cells (CRL-1586, ATCC). Cells were seeded at 1×10^6 cells/well in a 24-well Plate 18 h before virus transduction. Cells were incubated with the recombinant baculovirus under various MOI at 37 °C for 2 h. The unbound virus was then removed from cells. Cells were further cultured at 37 °C in fresh culture medium for 24–48 h before examination with fluorescence microscopy or analysis with flow cytometry.

2.4. Flow cytometric analysis

Cells (1×10^6 cells/well) were collected by centrifugation ($800 \times g$, 5 min). After decanting the supernatant, cells were resuspended in PBS with 1% BSA and incubated with fluorescence-labeled antibodies [phytoerythrin (PE)-Cy5-conjugated anti-CD19, PE-conjugated anti-CD11b, and/or PE-conjugated anti-CD3 (BD PharMingen, San Diego, CA)] on ice for 30 min. Cells were washed twice with PBS containing 0.1% BSA before brief fixation with 1% paraformaldehyde on ice. The number of antibody-labeled cells was then determined by flow cytometry (Beckman Coulter Cytomics™ FC500), and data were analyzed using machine-embedded CXP software.

2.5. Immunocytochemistry

Immunocytochemistry were performed as previously described (Chow et al., 2004). Cells were deposited onto slides using a Cytospin procedure. Slides were air dried for 20 min and fixed in cold methanol/acetone for 10 min. Following blockage of the endogenous peroxidase activity and nonspecific antibody binding sites with 3% H_2O_2/0.2% NaN_3 [15 min, room temperature (RT)] and 5% goat serum (10 min, RT), respectively, slides were incubated with monoclonal antibodies specific to human CD-68 (DAKO, Glostrup, Denmark) at RT for 90 min, before further treatment with LSAB2 (DAKO). Chromogenic development was processed with peroxidase-conjugated streptavidin and aminoethylcarbazole (Sigma, St. Louis, MO) solution. The slides were counterstained with hematoxylin before mounting with glycerol gelatin and coverslips. Cells with a crimson red precipitate were identified as positive.

2.6. Phagocytosis assay

Macrophages were collected as peritoneal exudate cells after washing mouse abdominal cavity with 5 mL cold sucrose solution (0.34 M) (Trepicchio et al., 1996). Adherent macrophages or transduced lymphoma cells were incubated with 0.5 μL of 1 μm red carboxylated FluroSpheres (Molecular Probes, Invitrogen Taiwan, Ltd., Taipei, Taiwan) at 37 °C for 1 h. After several washes with PBS, cells were fixed *in situ* with 2% paraformaldehyde at room temperature for 5 min before microscopic examination.

2.7. RNA preparation and oligonucleotide microarrays

B lymphoma cells (Toledo) were collected without transduction (0 h) or following transduction with either vAtEpGS688 for 12, 24, and 48 h, or vAtE for 48 h. RNA extraction has been described previously (Chen et al., 2006). Briefly, following RNA extraction, the amount of RNA was measured by a ND-1000 spectrophotometer (NanoDrop Technologies, Wilmington, DE) at OD_{260}. The samples were divided into individual aliquots for gene expression analysis on a microarray platform. The procedures for microarray analysis were performed following the manufacturer's protocols. Briefly, following synthesis of cRNA from total RNA, the probe RNA was amplified (Fluorescent Linear Amplification Kit, Agilent Technologies, Santa Clara, CA) and respectively labeled with Cy3-CTP or Cy5-CTP (PerkinElmer, Waltham, MA). cRNA of vAtEpGS688-treated cells was labeled with Cy5, and cRNA from control cells was labeled with Cy3. The Cy-labeled cRNA was then fragmented and hybridized to Agilent Whole Human Genome 4×44k oligo microarray (Agilent Technologies, Santa Clara, CA) at 60 °C for 17 h. The hybridized microarrays were scanned with an Agilent microarray scanner (Agilent Technologies, Santa Clara, CA) at OD_{535} for Cy3 and OD_{625} for Cy5. Scanned images were analyzed by Feature extraction software 8.1 (Agilent Technologies). After image analysis, data were normalized by a rank-consistency-filtering LOWESS method.

2.8. GeneSpring analysis

Microarray data were analyzed using GeneSpring GX 7.3.1 (Agilent Technologies). Defined data analysis algorithm was used with sequential steps listed below: Probes were filtered with "Present or Marginal flags" in each sample. The resulting 35,713 probes were selected for differential expression, and 5186 differentially expressed genes had at least 2-fold changes and $P < 0.05$ by error model. The differentially expressed genes were further analyzed with cluster analysis. Gene annotations and gene ontology (GO) classifications of each cluster were obtained with gene ontology annotation (the correlated genes were connected with a symbol) and Proteome slim.

3. Results

3.1. Transduction specificity of SARS-CoV spike-displayed recombinant baculovirus

We evaluated the transduction efficacy of SARS-CoV spike protein-displayed recombinant baculovirus (SSDRB), vAtEpGS688, which carried amino acids 17–688 of SARS-CoV spike protein on the surface of viral envelope and the enhanced green fluorescent protein (*EGFP*) gene in the viral genome (Chang et al., 2004), in isolated murine alveolar type II epithelial cells (type II pneumocytes or ATII cells) and alveolar epithelium-derived lung cancer cells. Once transduced, *EGFP* gene under the control of the CMV promoter would be expressed in mammalian cells for fluorescence detection (Chang et al., 2004). On the other hand, spike protein displayed on SSDRB was produced under the control of the *polyhedrin* promoter (Chang et al., 2004), which would not be expressed in mammalian cells. As anticipated, SSDRB effectively transduced ATII cells (Fig. 1A). As a vector control, vAtE, which did not express SARS-CoV spike protein on the surface of viral envelope, could not transduce ATII cells (Fig. 1A).

Subsequently, human lung adenocarcinoma (LADC) cell lines, H226 and A549, and a human squamous cell lung cancer cell line, H125, were tested for *in vitro* SSDRB transduction assay. Among these 3 lung cancer cell lines, SSDRB barely infected H125, a cell line derived from alveolar type I (ATI) epithelial cancer, but efficiently transduced ATII-derived lung cancer cells, H226 (Fig. 1B) and A549 (data not shown). H226 cells were derived from a nonsmoker lung cancer patient, whereas A549 cells were derived from a lung cancer patient who smoked (http://www.atcc.org). The transduction rate, which was based on the presence of $EGFP^+$ cells, correlated with viral load. The average transduction rate under 100 MOI was around 35% and 16%, respectively, for murine ATII cells and H226 at 24 h posttransduction. These results indicate that SSDRB can indeed transduce ATII cells and ATII-derived LADC cells.

3.2. Transduction activity of SSDRB in human B cells

We tested the transduction activity of SSDRB on peripheral WBCs. $EGFP^+$ fluorescence microscopy confirmed that SSDRB could transduce peripheral WBCs (Fig. 2A). The transduction rate (based on $EGFP^+$ cells) was similar at 24–48 h posttransduction. Many transduced cells remained alive for at least 5 days (Fig. 2B). To determine the type of WBC that could be transduced by SSDRB, we used anti-CD19-coated magnetic beads to isolate and enrich human B cells from peripheral WBC. The result showed that SSDRB-transduced human B cells (right panel of Fig. 2C). Interestingly, the appearance of $EGFP^+$ B cells was larger and more granular than that of normal B cells at 24 h posttransduction. Cell morphology shows the presence of macrophages (center and lower right panels of Fig. 2C). Transduction of CD19-negative WBC, on the other hand, was minimal (left panel of Fig. 2C). The average transduction rate of SSDRB (50 MOI) in human peripheral B ($CD19^+$) cells was 17.9%. In a representative flow cytometric analysis, about 17% of peripheral B cells were transduced by SSDRB (50 MOI) at 24 h posttransduction (Fig. 2D), which was much higher (over 5-fold) than that by vAtE vector (3.2% transduced). About 64% (10.9% of 17%) of these SSDRB-transduced (GFP-positive) peripheral B cells simultaneously expressed CD19 and the myelocytic marker Mac-1 (CD11b). In contrast, only 2.6% (2.2% of 83%) of SSDRB-untransduced (GFP negative) cells simultaneously expressed CD19 and Mac-1 (Fig. 2D).

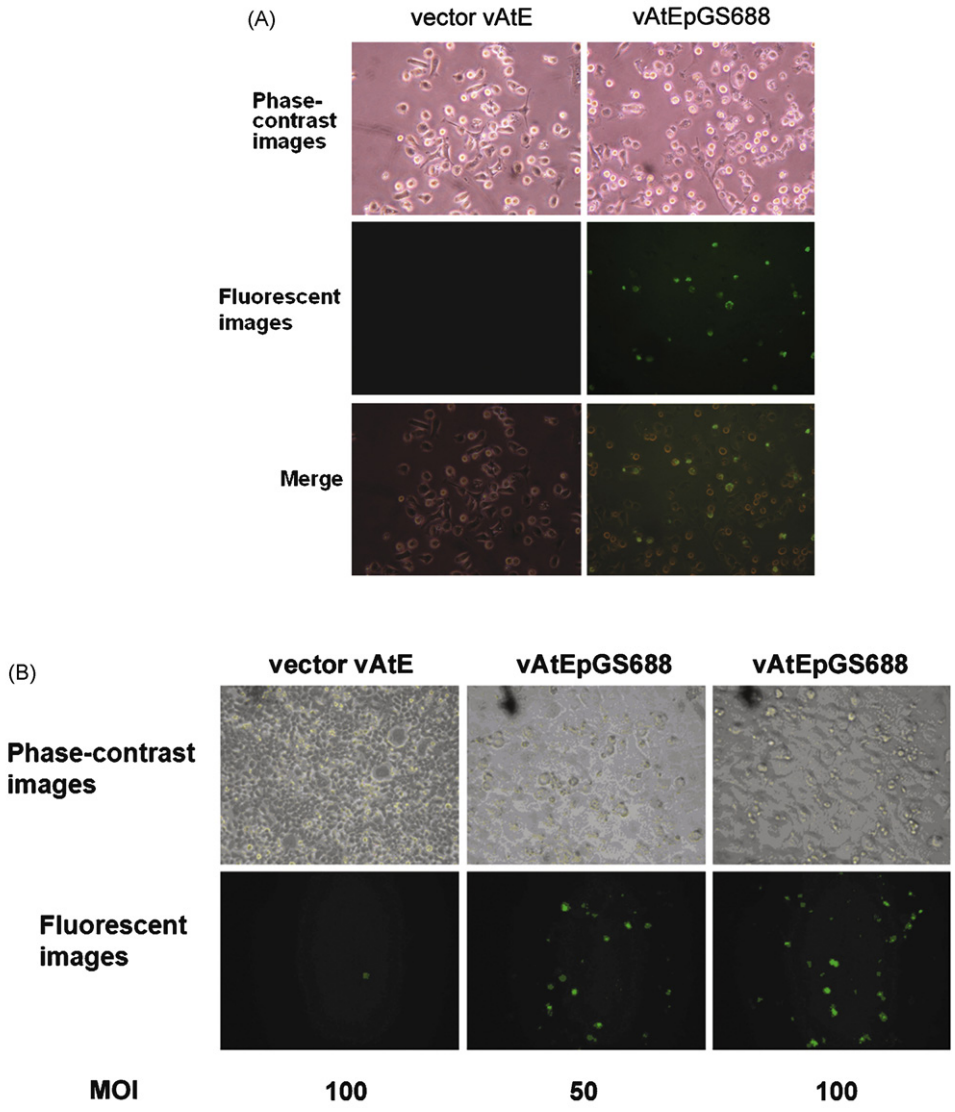

Fig. 1. Transduction specificity of SSDRB. (A) SSDRB (vAtEpGS688), which carried SARS-CoV spike protein on viral envelope and enhanced green fluorescent protein (EGFP) gene in viral genome, transduced isolated murine ATII cells. The average transduction rate at 100 MOI, as measured by the presence of $EGFP^+$ cells, was around 35%. (B) SSDRB (vAtEpGS688) transduced ATII-derived lung adenocarcinoma cells, H226. The average transduction rate at 100 MOI was 16%.

3.3. Conversion effect of SSDRB transduction on B lymphoma cells

To rule out the possibility that our observation was a result of the residual monocytes from the peripheral WBCs, we used B lymphoma cell lines, CA46, HT, and Toledo as the homogeneous B cells in the following studies. As shown by fluorescence microscopy, SSDRB-transduced all 3 B lymphoma cells (Fig. 3A). Interestingly, the appearance of SSDRB-transduced $EGFP^+$ cells was also larger and more granular than that of the control B lymphoma cells (without transduction or 0 h) (Fig. 3A). The transduction rate of SSDRB was dependent on viral load ($P<0.05$, $P<0.05$, and $P<0.001$ for CA46, HT, and Toledo cells, respectively) (Fig. 3B). In contrast, the transduction rate of vAtE control was minimum (Fig. 3B). The average transduction rate (based on $EGFP^+$ cells) of SSDRB (50 MOI) for CA46, HT, and Toledo cells at 24 h posttransduction was determined as 14.6%, 23.8%, and 33.9%, respectively (Fig. 3B). Results of flow cytometry revealed that a portion of SSDRB-transduced B cells could in fact express the myelocytic marker Mac-1 (CD11b). In a representative flow cytometric analysis, about 57.7% of SSDRB-transduced CA46 (9.4% of 16.3%) concurrently expressed Mac-1 and CD19 and 9.8% of them (1.6% of 16.3%) expressed Mac-1 only (GFP positive, lower right of Fig. 3C). In contrast, SSDRB-untransduced CA46 cells rarely expressed Mac-1 (0%) (GFP negative, right panel of Fig. 3C). Similar ratios were observed in HT cells (data not shown). On the other hand, 17.4% of SSDRB-transduced Toledo cells (5.6% of 32.1%) concurrently expressed Mac-1 and CD19, whereas 50.1% of them (16.1% of 32.1%) expressed Mac-1 exclusively (lower right of Fig. 3C). In sum, 67.5% of SSDRB-transduced CA46 or Toledo cells became Mac-1 positive. On the other hand, few (0.8% of 67.9%) SSDRB-untransduced Toledo cells expressed Mac-1 (GFP negative, right panel of Fig. 3C). As an untreated control, only 0.5% of CA46 and 0.9% of Toledo cells expressed Mac-1. As a vector control, vAtE treated-B lymphoma cells scarcely expressed Mac-1 (left panel of Fig. 3C). These data suggest that SSDRB could convert B cells into macrophage-like cells.

Immunocytochemical characterization showed that transduced B cells expressed the activated monocyte/macrophage-specific marker CD68 (stained in crimson red with aminoethylcarbazole) from 24 to 48 h posttransduction. These CD68-positive cells

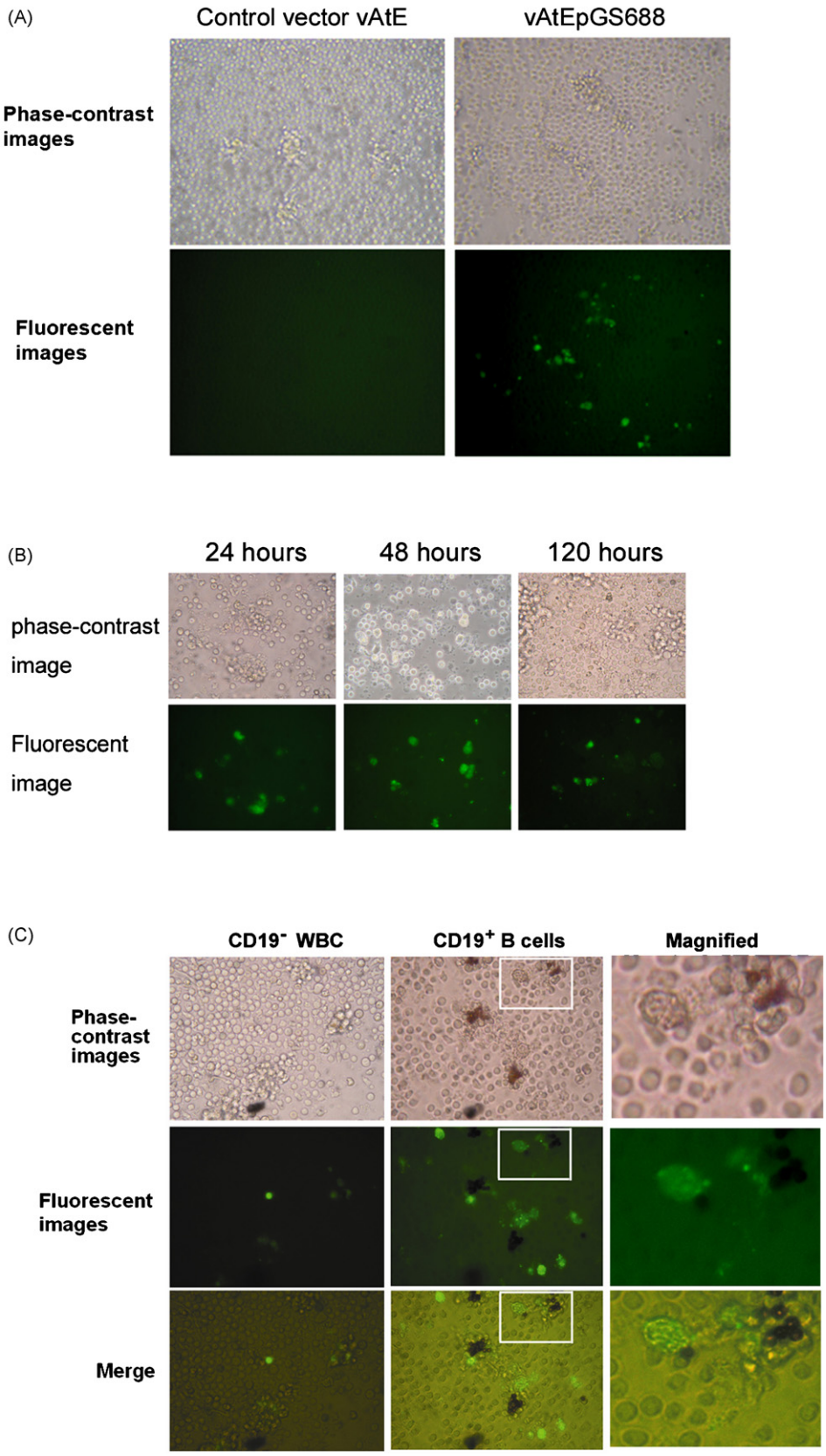

Fig. 2. SSDRB transduction of human peripheral B cells. (A) Peripheral white blood cells (WBCs) were transduced with SSDRB (50 MOI), and EGFP$^+$ transduced cells were observed by fluorescence microscopy. (B) Human WBCs were transduced with SSDRB (50 MOI) and observed by fluorescence microscopy at 24, 48, and 120 h, respectively. (C) SSDRB (50 MOI) transduced anti-CD19-magnetic bead-enriched human peripheral B cells (right panel). Transduction of CD19$^-$ WBCs was minimal (left panel). The appearance of EGFP$^+$ B cells was larger and more granular than that of normal B cells at 24 h posttransduction. Cell morphology was similar to that of macrophages (center and upper right panels). (D) Human peripheral B (CD19$^+$) cells were transduced with SSDRB (50 MOI), and analyzed by flow cytometry at 24 h posttransduction. Cells were gated for GFP fluorescence. Both transduced (GFP-positive) and untransduced (GFP negative) cells were analyzed for the expression of CD19 and Mac-1 (CD11b).

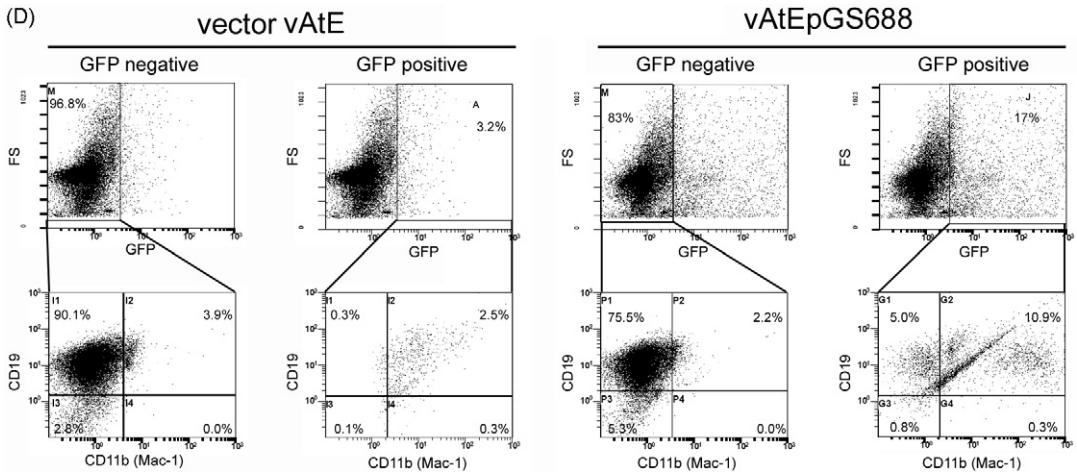

Fig. 2. (*Continued*).

continuously increased in size from 24 to 48 h and became morphologically similar to monocyte/macrophages with enlarged and horseshoe-shape nuclei (counterstained in blue with hematoxylin) (Fig. 3D).

3.4. SSDRB-mediated changes of gene expression patterns during conversion of B lymphoma cells

To determine SSDRB-mediated changes of gene expression profiles, oligonucleotide microarrays were used to identify genes that were expressed at 12, 24, and 48 h after SSDRB or 48 h after vAtE addition in Toledo cells. Gene expression profiles of Toledo cells harvested without induction were analyzed in parallel as the 0-h control. Following analyses of scatter plotting and hierarchical clustering (Fig. 4A), differentially expressed genes were identified. Results showed that expression of CD86 (B7-2), which is a marker of monocytic/dendritic lineage (Re et al., 2002), and hypoxia-inducible factor-1α (HIF1α) increased markedly within 12 h of SSDRB treatment. At 48 h after SSDRB addition, the level of CD86 and HIF1α increased to more than 4-fold and 2.5-fold, respectively. Expression of suppressor of cytokine signaling (SOCS or STAT-induced STAT inhibitor)-3, CCAAT/enhancer-binding protein beta (C/EBPβ), insulin-like growth factor-binding protein 3 (IGFBP3), Krüpple-like factor (KLF)-5, and CD54 (receptor for Mac-1) increased gradually around 24–48 h after SSDRB treatment (Fig. 4B). On the other hand, vAtE control did not show apparent enhancement in these gene expression profiles (Fig. 4C).

In this study, we observed SSDRB-mediated upregulation of HIF-1α during conversion of B lymphoma cells. Because HIF-1α has been known to correlate with phagocytosis activity of macrophages under hypoxic conditions (Anand et al., 2007), we thereby investigated whether hypoxia could have any effect on the conversion of B lymphoma cells into macrophage-like cells. Interestingly, following exposure to hypoxia for 16–24 h (in an incubation chamber with 5% CO_2 and 95% nitrogen), size and morphology of B lymphoma cells changed markedly and bore a resemblance to monocytes/macrophages with enlarged and horseshoe-shape nuclei. These macrophage-like cells were positive for CD68 (Fig. 5A) and could readily ingest recombinant SARS spike proteins (RSSP) 24 h posthypoxia (data not shown). However, unlike macrophages isolated from mouse peritoneal cavity, these cells did not readily adhere to plates nor engulfed red fluorescent beads. Likewise, SSDRB-transduced B lymphoma cells (Toledo) ($EGFP^+$ cells) could hardly engulf any red fluorescent beads (microspheres) under both normoxia and hypoxia exposures (Fig. 5B and C).

4. Discussion

In previous studies, we and others have demonstrated that type II pneumocytes and macrophages are the target cells of SARS-CoV in the lung (Chow et al., 2004; Ding et al., 2004; Gu et al., 2005; Shieh et al., 2005). In this study, we showed that SSDRB could indeed transduce mouse type II pneumocytes (ATII cells) and ATII-derived cancer cells (H-226) (Fig. 1), indicating that SSDRB can bind to and enter target cells of SARS-CoV. Our results further indicate that spike protein displayed on SSDRB can indeed trigger the conversion of peripheral B cells and B lymphoma cells into macrophage-like cells. Among 3 B lymphoma cell lines, transduced CA46 and HT cells could concurrently express Mac-1 and CD19, whereas transduced Toledo cells mainly expressed Mac-1. In addition, conversion of B cells into macrophage-like cells could also take place under severe hypoxia, a compounded condition of SARS infection. Our data provide a reasonable explanation for the reduced B lymphocytes and the profusely infiltrated macrophages in SARS patients, in whom the newly emerged macrophages in the infected lung expressed B-cell markers (Chow et al., 2004). In contrast to B cells, we observed a very low transduction rate on CD19-negative WBC (left panel of Fig. 2B), indicating that peripheral T lymphocytes were not the target for SSDRB.

Pathologically, expression of bilineage markers for both neutrophils and monocytes, or that of mixed-lineage markers for both lymphocytes and monocytes, has been found in a subtype of acute myelocytic leukemia, M4, or non-Hodgkin's lymphoma (Horny et al., 1994; Umiel et al., 1993). Coexpression of B-cell and macrophage markers, e.g., Mac-1 (CD11b), CD14, CD15, CD19, CD20, and CD68, has been found in Hodgkin's and Reed–Sternberg (RS) cells of Hodgkin's lymphoma (HL) (Hsu et al., 1990; Zukerberg et al., 1991). Malignant HL cells behave like macrophages *in vitro*, engulfing exogenously added *Candida albicans* (Hsu et al., 1990). Moreover, among HL subtypes, including lymphocyte predominance, mixed cellularity, nodular sclerosis, and lymphocyte depletion, reduction of lymphocytes is correlated with poorer prognosis of the disease (Shimabukuro-Vornhagen et al., 2005). Interestingly, Epstein-Barr virus (EBV) is frequently detected in HL lesions (Weiss et al., 1987) and EBV infection is also associated with disease progression (Claviez et al., 2005; Keegan et al., 2005), particularly in older patients with nodular sclerosis and lymphocyte depletion. Based on these data and our current results, we propose that virus infection, such as EBV and SARS, may take a shortcut in accelerating unusual conversion of lymphocytes to macrophage-like cells under severe conditions, in which the patient's immune system may not be able to respond in time

to neutralize viral infection either humorally or cellularly (Ding et al., 2003).

As determined by microarray analysis, expression of *CD86* (B7-2) gene was rapidly induced in B lymphoma cells within 12 h of SSDRB treatment (Fig. 4B). This result suggests that SSDRB-transduced B lymphoma cells were redirected to express marker of monocytic/dendritic lineage (Re et al., 2002). Likewise, *HIF1α* gene expression was induced within 12 h of SSDRB treatment. Interestingly, expression of *HIF1α* has been known to correlate with increased phagocytic activity of macrophages under hypoxia

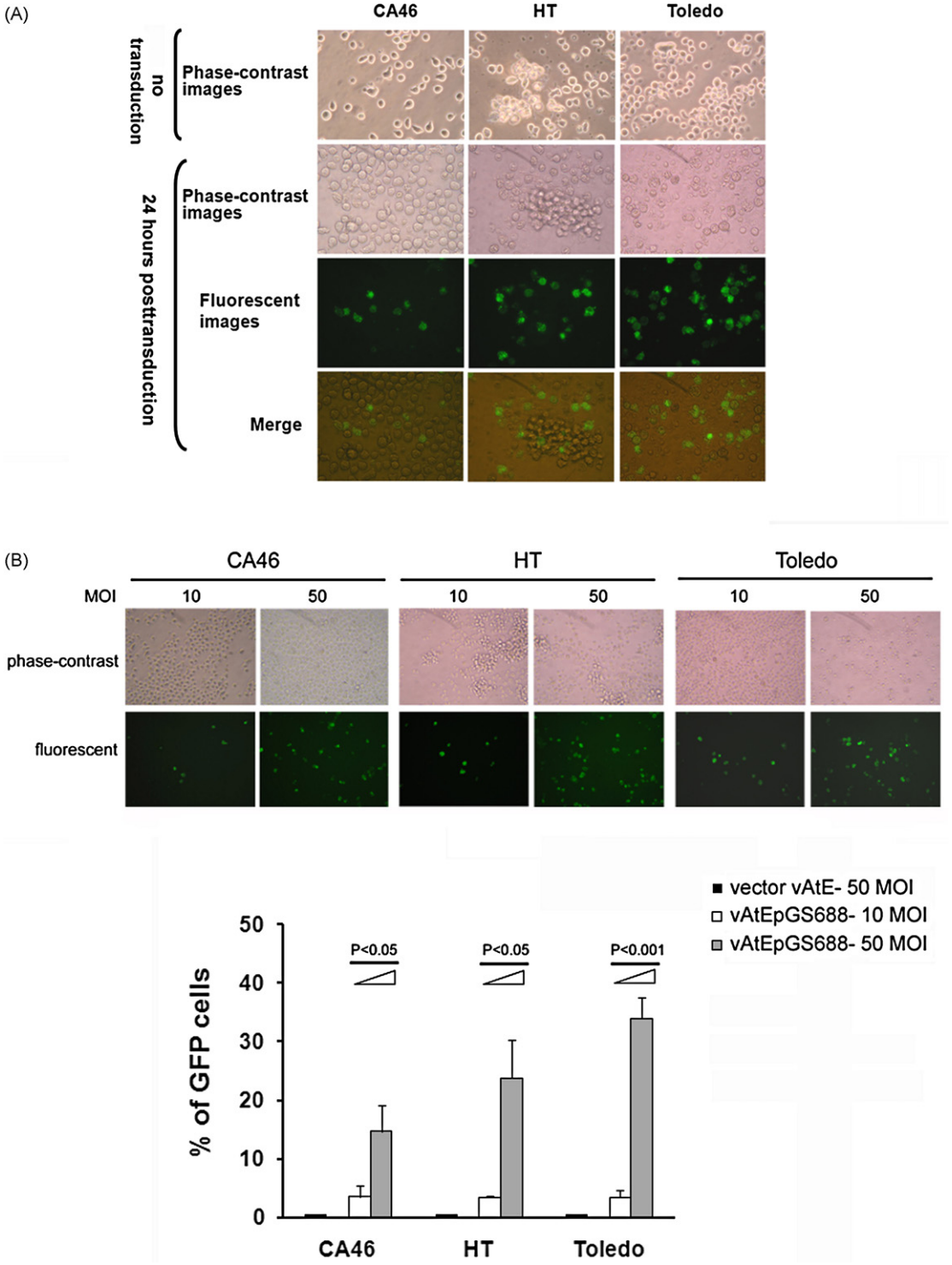

Fig. 3. SSDRB transduction-induced conversion of B lymphoma cells into macrophages. (A) As shown by fluorescence microscopy, SSDRB (50 MOI) transduced B lymphoma cells, CA46, HT, and Toledo. The appearance of EGFP$^+$ cells was larger and more granular than that of the untransduced B lymphoma cells. (B) B lymphoma cells were transduced with SSDRB at 10 and 50 MOI, respectively. (C) SSDRB-treated CA46 and Toledo cells were analyzed by flow cytometry for the expression of Mac-1 and CD19 at 24 h posttransduction. SSDRB-treated cells were gated for GFP fluorescence (right panel). (D) Immunocytochemical characterization showed that transduced B lymphoma cells expressed the macrophage-specific marker CD68 from 24 to 48 h. These CD68-positive cells continuously increased in size from 24 to 48 h, and became morphologically like monocyte/macrophages with enlarged and horseshoe-shape nuclei (counterstained in blue with hematoxylin) (arrowhead). White arrow indicates an untransduced B lymphoma cell. Each experiment was repeated at least 3 times.

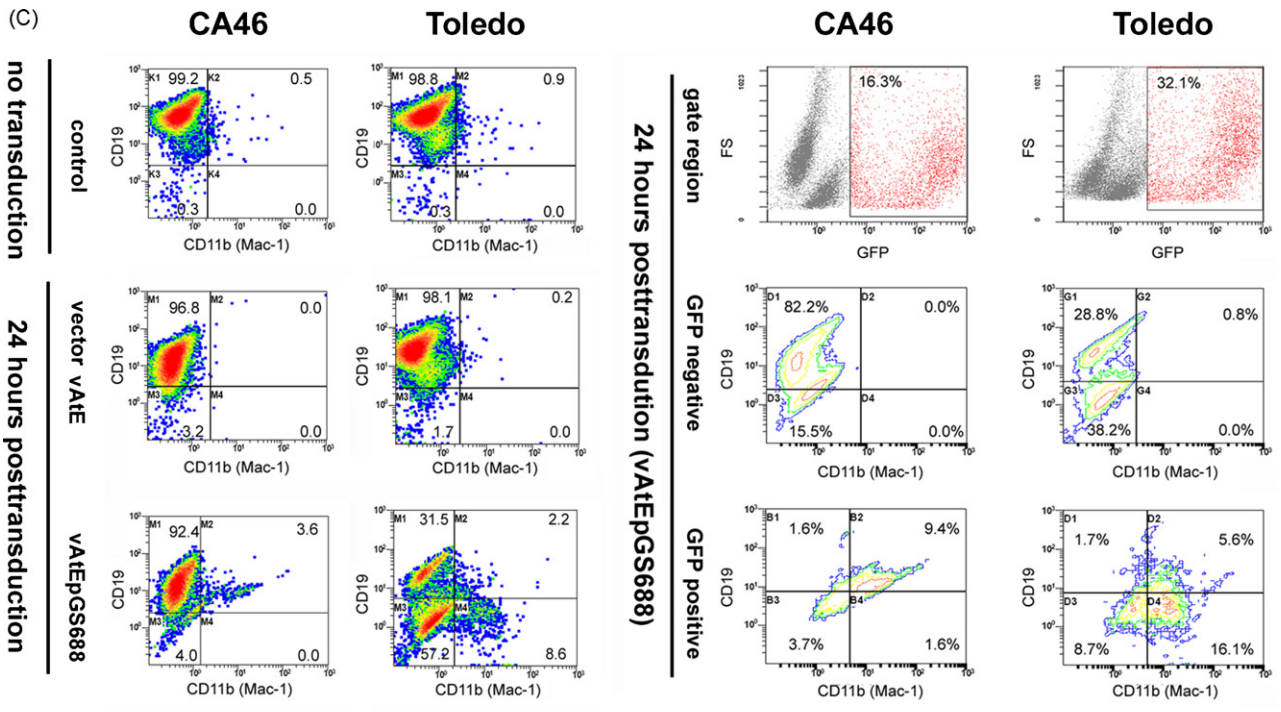

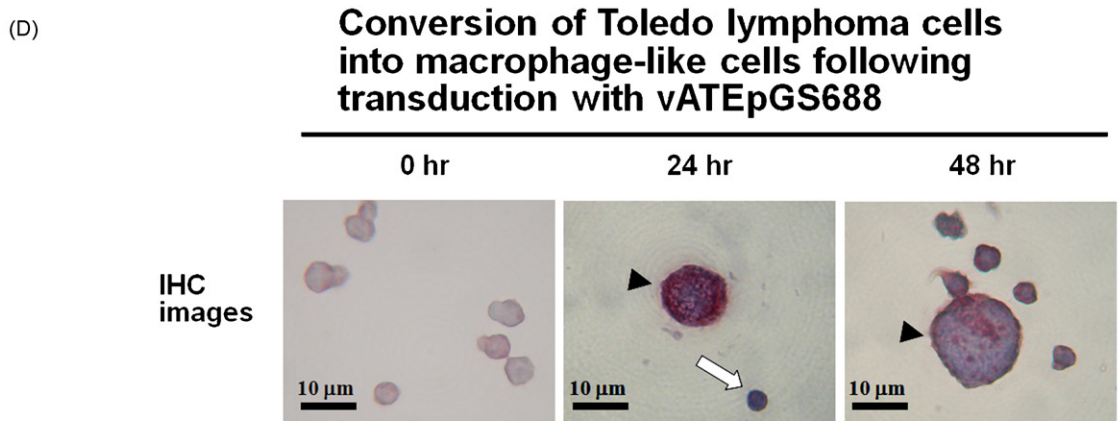

Fig. 3. (*Continued*).

(Anand et al., 2007). Besides SSDRB, prolonged exposure to hypoxia also induced conversion of B cells to macrophage-like cells (Fig. 5A). SSDRB and hypoxia may somehow interact synergistically to induce phenotype conversion (Fig. 5B). Taken together, we have identified the Mac-1 marker (macrophage specific) (Fig. 2D and 3C), CD68 marker (monocyte/macrophage specific) (Fig. 3D), and CD86 marker (for monocytic/dendritic lineage) (Fig. 4B) in these macrophage-like cells converted from SSDRB-transduced B cells. Nonetheless, these macrophage-like cells might not readily function as normal macrophages since they did not adhere well to plates nor efficiently engulfed red fluorescent beads (Fig. 5B and C). Therefore, such phenotypic conversion could be a pathological effect rather than a host-protective response.

Enhanced expression of C/EBPβ in SSDRB-transduced B lymphoma cells was observed around 24–48 h after SSDRB treatment. Notably, several previous studies reported that ectopic expression of transcription factors, either C/EBPβ plus C/EBPα or PU.1 alone, initiated phenotypic conversion of B cells into macrophages (Orkin, 2000; Sieweke and Graf, 1998; Xie et al., 2004). In our study, levels of C/EBPα and PU.1 gene expression were not significantly different after SSDRB transduction. Instead, 2 other transcription factors, HIF1α and KLF-5, were found upregulated in SSDRB-transduced B lymphoma cells (Fig. 4B). In the future, it would be necessary to determine whether HIF1α and KLF-5 may interact together with C/EBPβ or act independently to participate in the conversion of B cells into macrophage-like cells. Grutkoski et al. (2003) has reported that SOCS-3 is induced exclusively in macrophages of septic mice to suppress inflammatory response. Here, we observed upregulated *SOCS-3* gene expression around 24–48 h after SSDRB treatment, suggesting that macrophage-like cells converted from B cells might block inflammatory signaling via SOCS-3 action. In addition, our microarray analysis showed an increased expression in CD54 after SSDRB treatment. Interestingly, CD54 and Mac-1 upregulation is known to be related to the transmigration of peripheral monocytes and their differentiation into peritoneal macrophages (Liberek et al., 2004). In our study, upregulation of CD54 (by microarray) and Mac-1 (by flow cytometry) correlated well with the conversion into macrophage-like cells. This result suggests that these macrophage-like cells may possess transmigration ability. Moreover, IGFBP3 was induced after SSDRB treatment. IGFBP3 may

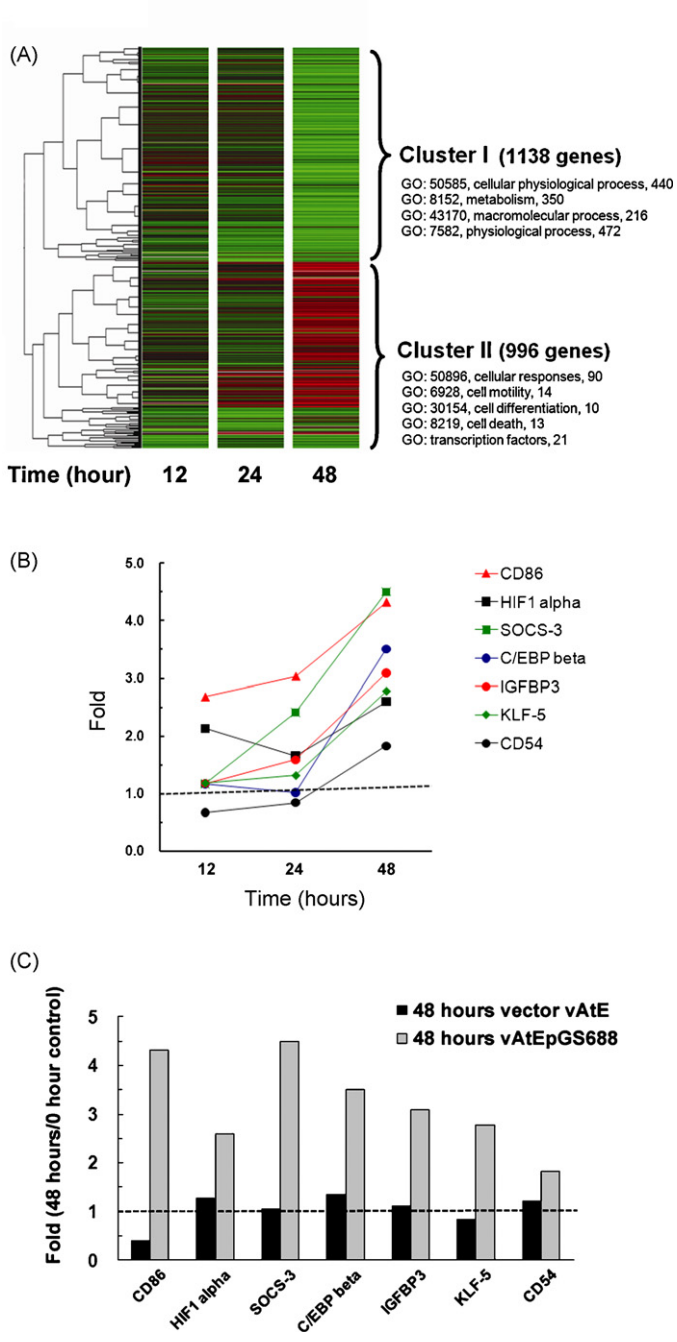

Fig. 4. SSDRB-mediated changes of gene expression profiles in B lymphoma cells. Microarray was used to identify genes that were expressed in Toledo cells after SSDRB (50 MOI) transduction. (A) Following analyses of scatter plotting and hierarchical clustering, differentially expressed genes were identified. Red indicates genes that were upregulated. Green indicates genes that were downregulated. Unchanged genes were shown in black. (B) Expression of CD86 and HIF1α increased markedly within 12 h of SSDRB treatment. At 48 h after SSDRB addition, the level of CD86 and HIF1α increased to more than 4-fold and 2.5-fold, respectively. Expression of SOCS-3, C/EBPβ, IGFBP3, KLF-5, and CD54 increased gradually around 24–48 h after SSDRB treatment. (C) Folds of gene enhancement (48 h vs. 0 h) were compared between SSDRB-treated cells and vAtE control. Each experiment was repeated at least 3 times.

function either as an antiapoptotic or proapoptotic factor depending on the cell type and condition (Granata et al., 2004). Wilson et al. (2005) has reported that IGFBP3 may protect myeloid cells against apoptosis mediated by Fas ligand or tumor necrosis factor alpha (TNFα). Accordingly, IGFBP3 could protect macrophage-like cells from apoptosis. As shown in Fig. 4A, several genes that may be involved in cell death were differentially expressed after SSDRB treatment. Nonetheless, many of them were not significantly different until 48 h posttransduction. Among 6 genes that were upregulated at 48 h posttransduction, 3 encoded antiapoptotic factors (*GADD45B*, *BAG-3*, *osteopontin*) (Gupta et al., 2006; Liao et al., 2001; Song et al., 2008) and 3 encoded apoptotic factors (*galectin-1*, *Fas*, and *DEDD2*) (Kovács-Sólyom et al., 2010; Itoh et al., 1991; Alcivar et al., 2003) (data not shown). By flow cytometry, we observed a small fraction of SSDRB-treated cells in the sub-G1 phase (data not shown), which may represent apoptotic cells and could explain in part the lymphopenia observed in SARS patients (Chow et al., 2004; Nicholls et al., 2003; Zhan et al., 2006). However, given the fact that the percentage of sub-G1 cells was much lower than the transduction rate, and around two-thirds of SSDRB-transduced cells became Mac-1 positive, we expect that macrophage-like cells converted from B cells may not represent dying proapoptotic cells. Finally, these macrophage-like cells (Figs. 3D and 5A) did not show any apoptotic features such as shrinkage in morphology, nuclear condensation, or apoptotic bodies (Kerr et al., 1972; Rich et al., 1999).

Certain murine B-cell lines have been reported to be able to transform into macrophage-like cells without ectopic overexpression of transcription factors (Tanaka et al., 1994; Spencker et al., 1995). Among them, a nonadherent pre-B-cell line, 70Z/3, is known to be able to transform into an adherent pre-B-cell lineage and from which a macrophage-like lineage can be generated spontaneously without any known ligand (Tanaka et al., 1994). However, transition from an adherent pre-B subclone of 70Z/3 to macrophage-like lineage takes about 1 month. On the other hand, $CD5^+$ pre-B or B1 cell lines (e.g., SPGM-1, TH2.52) can be converted into macrophage-like cells from 1 to 3 days upon induction with ligands such as phorbol ester/calcium ionophore or interferon-gamma (IFN-γ) (Spencker et al., 1995; Koide et al., 2002). In our study, we also observed a fast transition (within 1–2 days posttransduction) from peripheral B cells or B lymphoma cells to macrophage-like cells after stimulation with spike protein of SARS displayed on recombinant baculovirus. Addition of recombinant spike protein, in contrast, did not result in such phenotypic transition (data not shown). It is likely that spike protein displayed on recombinant baculovirus adopts a similar conformation as that on SARS-CoV. However, we should point out that the experiments presented here were done with a spike-expressing recombinant virus instead of SARS-CoV. In the future, it is imperative to elucidate whether SARS-CoV or other viruses may induce B cell conversion.

Undoubtedly, all these observations may have other interpretations (Chang et al., 2004; Chow et al., 2004), and the impact of SARS infection on lymphocyte conversion and delayed immune responses remains to be clarified. Although other gene products of SARS virus could be associated with the pulmonary pathology (Chow et al., 2004; Ding et al., 2003), it is clear that spike protein, either directly or indirectly, affects lymphocyte conversion to myeloid cells, in particular if the viral effect is pathologically combined with hypoxia, which is an inevitable consequence of SARS infection. This in and of itself should provide a tool for elucidating the mechanism of delayed immune responses resulting from virus infection, and the subsequent pulmonary pathology and fatality (Chow et al., 2004; Ding et al., 2003), of which the clinical symptoms are similar to those seen in patients infected with the avian influenza virus H5N1 (Ng et al., 2006). It is possible that conversion of B cells to macrophage-like cells could be general during malicious virus infection, and such immediate host response could become more devastating than the routine immune response.

In conclusion, we show that spike protein of SARS displayed on recombinant baculovirus or prolonged exposure to hypoxia can trigger the conversion of peripheral B cells and B lym-

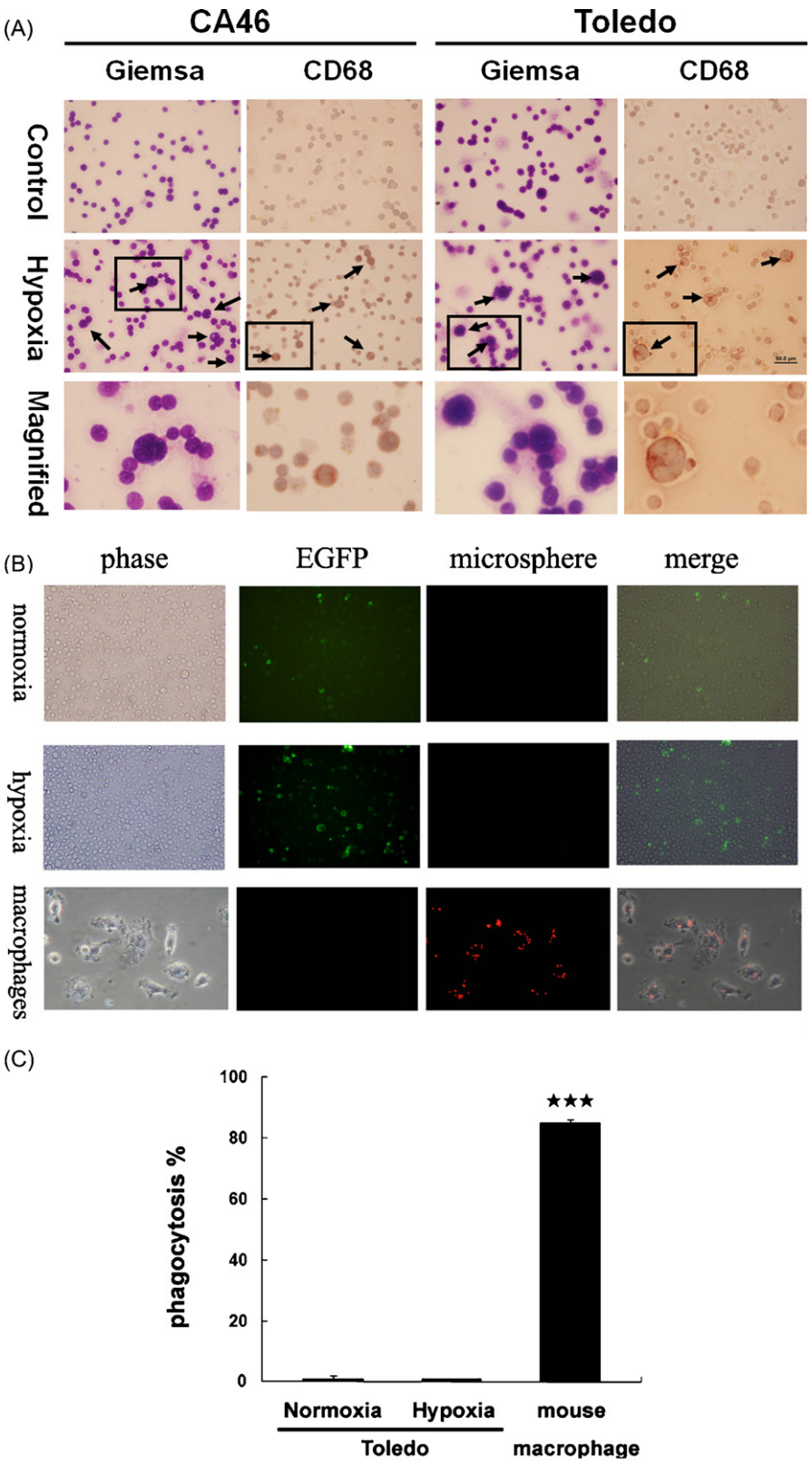

Fig. 5. Exposure to hypoxia induces conversion of B lymphoma cells to macrophages. (A) Following exposure to hypoxia (in an incubation chamber with 5% CO_2 and 95% nitrogen) for 16–24 h, the size of some B lymphoma cells (as determined by Giemsa stain), both CA46 and Toledo, was increased markedly (indicated by arrows). Cell morphology of enlarged cells resembled that of monocytes/macrophages with horseshoe-shape nuclei. These cells were immunologically positive for CD68. (B) SSDRB-transduced B lymphoma cells (Toledo) ($EGFP^+$ cells) could hardly engulf any red fluorescent beads (microspheres) under both normoxia and hypoxia exposures. In contrast, macrophages isolated from mouse peritoneal cavity could readily ingest red fluorescent microspheres with high efficiency. (C) Phagocytosis percentage (%) of SSDRB-transduced B lymphoma cells (Toledo) under normoxia or hypoxia was determined, respectively, as the percentage of cells positive with more than 2 internalized microspheres. ***Significantly different ($P < 0.001$). Each experiment was repeated at least 3 times.

phoma cells into Mac-1 positive macrophage-like cells. This is the first time a viral protein is identified as a ligand for phenotype conversion of B cells. Spike protein of SARS or hypoxia treatment may provide the convenient platform for studying signaling pathways involved in leukocyte interconversion or differentiation.

Acknowledgements

We thank Dr. Y.-C. Chao (Institute of Molecular Biology, Academia Sinica, Nankang, Taipei, Taiwan) for providing us recombinant baculovirus vAtEpGS688.

References

Akashi, K., Traver, D., Miyamoto, T., Weissman, I.L., 2000. A clonogenic common myeloid progenitor that gives rise to all myeloid lineages. Nature 404, 193–197.
Alcivar, A., Hu, S., Tang, J., Yang, X., 2003. DEDD and DEDD2 associate with caspase-8/10 and signal cell death. Oncogene 22, 291–297.
Alexander, W.S., 1998. Cytokines in hematopoiesis. Int. Rev. Immunol. 16, 651–682.
Anand, R.J., Gribar, S.C., Li, J., Kohler, J.W., Branca, M.F., Dubowski, T., Sodhi, C.P., Hackam, D.J., 2007. Hypoxia causes an increase in phagocytosis by macrophages in a HIF-1α-dependent manner. J. Leukoc. Biol. 82, 1257–1265.
Chang, Y.J., Liu, C.Y., Chiang, B.L., Chao, Y.C., Chen, C.C., 2004. Induction of IL-8 release in lung cells via activator protein-1 by recombinant baculovirus displaying severe acute respiratory syndrome-coronavirus spike proteins: identification of two functional regions. J. Immunol. 173, 7602–7614.
Chen, J.T., Lin, T.S., Chow, K.C., Huang, H.H., Chiou, S.H., Chiang, S.F., Chen, H.C., Chuang, T.L., Lin, T.Y., Chen, C.Y., 2006. Cigarette smoking induces overexpression of HGF in type II pneumocytes and lung cancer cells. Am. J. Respir. Cell Mol. Biol. 34, 264–273.
Chiu, C.F., Chow, K.C., Lin, T.Y., Tsai, M.H., Shih, C.M., Chen, L.M., 2000. Involvement of virus infection in patients with histiocytic necrotizing lymphadenitis in Taiwan—detection of Epstein-Barr virus, type I human T-cell lymphotropic virus and parvovirus B19. Am. J. Clin. Pathol. 113, 774–781.
Chow, K.C., Hsiao, C.H., Lin, T.Y., Chen, C.L., Chiou, S.H., 2004. Detection of severe acute respiratory syndrome-associated coronavirus in pneumocytes of the lung. Am. J. Clin. Pathol. 121, 574–580.
Claviez, A., Tiemann, M., Lüders, H., Krams, M., Parwaresch, R., Schellong, G., Dörffel, W., 2005. Impact of latent Epstein-Barr virus infection on outcome in children and adolescents with Hodgkin's lymphoma. J. Clin. Oncol. 23, 4048–4056.
Corti, M., Brody, A.R., Harrison, J.H., 1996. Isolation and primary culture of murine alveolar type II cells. Am. J. Respir. Cell Mol. Biol. 14, 309–315.
Ding, Y., Wang, H., Shen, H., Li, Z., Geng, J., Han, H., Cai, J., Li, X., Kang, W., Weng, D., Lu, Y., Wu, D., He, L., Yao, K., 2003. The clinical pathology of severe acute respiratory syndrome (SARS): a report from China. J. Pathol. 200, 282–289.
Ding, Y., He, L., Zhang, Q., Huang, Z., Che, X., Hou, J., Wang, H., Shen, H., Qiu, L., Li, Z., Geng, J., Cai, J., Han, H., Li, X., Kang, W., Weng, D., Liang, P., Jiang, S., 2004. Organ distribution of severe acute respiratory syndrome (SARS) associated coronavirus (SARS-CoV) in SARS patients: implications for pathogenesis and virus transmission pathways. J. Pathol. 203, 622–630.
Granata, R., Trovato, L., Garbarino, G., Taliano, M., Ponti, R., Sala, G., Ghidoni, R., Ghigo, E., 2004. Dual effects of IGFBP-3 on endothelial cell apoptosis and survival: involvement of the sphingolipid signaling pathways. FASEB J. 18, 1456–1458.
Grutkoski, P.S., Chen, Y., Chung, C.S., Ayala, A., 2003. Sepsis-induced SOCS-3 expression is immunologically restricted to phagocytes. J. Leukoc. Biol. 74, 916–922.
Gu, J., Gong, E., Zhang, B., Zheng, J., Gao, Z., Zhong, Y., Zou, W., Zhan, J., Wang, S., Xie, Z., Zhuang, H., Wu, B., Zhong, H., Shao, H., Fang, W., Gao, D., Pei, F., Li, X., He, Z., Xu, D., Shi, X., Anderson, V.M., Leong, A.S., 2005. Multiple organ infection and the pathogenesis of SARS. J. Exp. Med. 202, 415–424.
Gupta, M., Gupta, S.K., Hoffman, B., Liebermann, D.A., 2006. Gadd45a and Gadd45b protect hematopoietic cells from UV-induced apoptosis via distinct signaling pathways, including p38 activation and JNK inhibition. J. Biol. Chem. 281, 17552–17558.
Heyworth, C., Pearson, S., May, G., Enver, T., 2002. Transcription factor-mediated lineage switching reveals plasticity in primary committed progenitor cells. EMBO J. 21, 3770–3781.
Horny, H.P., Wehrmann, M., Steinke, B., Kaiserling, E., 1994. Assessment of the value of immunohistochemistry in the subtyping of acute leukemia on routinely processed bone marrow biopsy specimens with particular reference to macrophage-associated antibodies. Hum. Pathol. 25, 810–814.
Hsu, S.M., Xie, S.S., Hsu, P.L., 1990. Cultured Reed–Sternberg cells HDLM-1 and KM-H2 can be induced to become histiocyte-like cells. H-RS cells are not derived from lymphocytes. Am. J. Pathol. 137, 353–367.
Itoh, N., Yonehara, S., Ishii, A., Yonehara, M., Mizushima, S., Sameshima, M., Hase, A., Seto, Y., Nagata, S., 1991. The polypeptide encoded by the cDNA for human cell surface antigen Fas can mediate apoptosis. Cell 66, 233–243.
Keegan, T.H., Glaser, S.L., Clarke, C.A., Gulley, M.L., Craig, F.E., Digiuseppe, J.A., Dorfman, R.F., Mann, R.B., Ambinder, R.F., 2005. Epstein-Barr virus as a marker of survival after Hodgkin's lymphoma: a population-based study. J. Clin. Oncol. 23, 7604–7613.
Kerr, J.F.R., Wyllie, A.H., Currie, A.R., 1972. Apoptosis: a basic biological phenomenon with wide ranging implications in tissue kinetics. Br. J. Cancer 26, 239–257.
Koide, N., Sugiyama, T., Mori, I., Mu, M.M., Hamano, T., Yoshida, T., Yokochi, T., 2002. Change of mouse CD5$^+$ B1 cells to a macrophage-like morphology induced by gamma interferon and inhibited by interleukin-4. Clin. Diagn. Lab. Immunol. 9, 1169–1174.
Kovács-Sólyom, F., Blaskó, A., Fajka-Boja, R., Katona, R.L., Végh, L., Novák, J., Szebeni, G.J., Krenács, L., Uher, F., Tubak, V., Kiss, R., Monostori, E., 2010. Mechanism of tumor cell-induced T-cell apoptosis mediated by galectin-1. Immunol. Lett. 127, 108–118.
Laslo, P., Spooner, C.J., Warmflash, A., Lancki, D.W., Lee, H.J., Sciammas, R., Gantner, B.N., Dinner, A.R., Singh, H., 2006. Multilineage transcriptional priming and determination of alternate hematopoietic cell fates. Cell 126, 755–766.
Loose, M., Patient, R., 2006. Global genetic regulatory networks controlling hematopoietic cell fates. Curr. Opin. Hematol. 13, 229–236.
Liao, Q., Ozawa, F., Friess, H., Zimmermann, A., Takayama, S., Reed, J.C., Kleeff, J., Büchler, M.W., 2001. The anti-apoptotic protein BAG-3 is overexpressed in pancreatic cancer and induced by heat stress in pancreatic cancer cell lines. FEBS Lett. 503, 151–157.
Liberek, T., Chmielewski, M., Lichodziejewska-Niemierko, M., Lewandowski, K., Rutkowski, B., 2004. Transmigration of blood leukocytes into the peritoneal cavity is related to the upregulation of ICAM-1 (CD54) and Mac-1 (CD11b/CD18) adhesion molecules. Perit. Dial. Int. 24, 139–146.
Nakajima, H., Kizaki, M., Sonoda, A., Mori, S., Harigaya, K., Ikeda, Y., 1994. Retinoids (all-trans and 9-cis retinoic acid) stimulate production of macrophage colony-stimulating factor and granulocyte-macrophage colony-stimulating factor by human bone marrow stromal cells. Blood 84, 4107–4115.
Ng, W.F., To, K.F., Lam, W.W., Ng, T.K., Lee, K.C., 2006. The comparative pathology of severe acute respiratory syndrome and avian influenza A subtype H5N1—a review. Hum. Pathol. 37, 381–390.
Nicholls, J.M., Poon, L.L., Lee, K.C., Ng, W.F., Lai, S.T., Leung, C.Y., Chu, C.M., Hui, P.K., Mak, K.L., Lim, W., Yan, K.W., Chan, K.H., Tsang, N.C., Guan, Y., Yuen, K.Y., Peiris, J.S., 2003. Lung pathology of fatal severe acute respiratory syndrome. Lancet 361, 1773–1778.
Orkin, S.H., 2000. Diversification of haematopoietic stem cells to specific lineages. Nat. Rev. Genet. 1, 57–64.
Rich, T., Watson, C.J., Wyllie, A., 1999. Apoptosis: the germs of death. Nat. Cell Biol. 1, E69–E71.
Reddy, V.A., Iwama, A., Iotzova, G., Schulz, M., Elsasser, A., Vangala, R.K., Tenen, D.G., Hiddemann, W., Behre, G., 2002. Granulocyte inducer C/EBPalpha inactivates the myeloid master regulator PU.1: possible role in lineage commitment decisions. Blood 100, 483–490.
Re, F., Arpinati, M., Testoni, N., Ricci, P., Terragna, C., Preda, P., Ruggeri, D., Senese, B., Chirumbolo, G., Martelli, V., Urbini, B., Baccarani, M., Tura, S., Rondelli, D., 2002. Expression of CD86 in acute myelogenous leukemia is a marker of dendritic/monocytic lineage. Exp. Hematol. 30, 126–134.
Shieh, W.J., Hsiao, C.H., Paddock, C.D., Guarner, J., Goldsmith, C.S., Tatti, K., Packard, M., Mueller, L., Wu, M.Z., Rollin, P., Su, I.J., Zaki, S.R., 2005. Immunohistochemical, in situ hybridization, and ultrastructural localization of SARS-associated coronavirus in lung of a fatal case of severe acute respiratory syndrome in Taiwan. Hum. Pathol. 36, 303–309.
Shimabukuro-Vornhagen, A., Haverkamp, H., Engert, A., Balleisen, L., Majunke, P., Heil, G., Eich, H.T., Stein, H., Diehl, V., Josting, A., 2005. Lymphocyte-rich classical Hodgkin's lymphoma: clinical presentation and treatment outcome in 100 patients treated within German Hodgkin's Study Group trials. J. Clin. Oncol. 23, 5739–5745.
Sieweke, M.H., Graf, T., 1998. A transcription factor party during blood cell differentiation. Curr. Opin. Genet. Dev. 8, 545–551.
Song, G., Ming, Y., Mao, Y., Bao, S., Ouyang, G., 2008. Osteopontin prevents curcumin-induced apoptosis and promotes survival through Akt activation via alpha v beta 3 integrins in human gastric cancer cells. Exp. Biol. Med. 233, 1537–1545.
Spencker, T., Neumann, D., Strasser, A., Resch, K., Martin, M., 1995. Lineage switch of a mouse pre-B-cell line (SPMG-1) to macrophage-like cells after incubation with phorbol ester and calcium ionophore. Biochem. Biophys. Res. Commun. 216, 540–548.
Stanley, E.R., Jubinsky, P.T., 1984. Factors affecting the growth and differentiation of haemopoietic cells in culture. Clin. Hematol. 13, 329–348.
Tanaka, T., Wu, G.E., Paige, C.J., 1994. Characterization of the B cell-macrophage lineage transition in 70Z/3 cells. Eur. J. Immunol. 24, 1544–1548.
Trepicchio, W.L., Bozza, M., Pedneault, G., 1996. Recombinant human IL-11 attenuates the inflammatory response through down-regulation of proinflammatory cytokine release and nitric oxide production. J. Immunol. 157, 3627–3634.
Umiel, T., Pattengale, P., Weinberg, K., 1993. Recombination activating gene-1 (RAG-1) expression in all differentiation stages of B-lineage precursor acute lymphoblastic leukemia. Leukemia 7, 435–440.
Wang, D., D'Costa, J., Civin, C.I., Friedman, A.D., 2006. C/EBPalpha directs monocytic commitment of primary myeloid progenitors. Blood 108, 1223–1229.
Weiss, L.M., Strickler, J.G., Warnke, R.A., Purtilo, D.T., Sklar, J., 1987. Epstein-Barr viral DNA in tissues of Hodgkin's disease. Am. J. Pathol. 129, 86–91.

Wilson, H.M., Lesnikov, V., Plymate, S.R., Ward, J., Deeg, H.J., 2005. High IGFBP-3 levels in marrow plasma in early-stage MDS: effects on apoptosis and hemopoiesis. Leukemia 19, 580–585.
Xie, H., Ye, M., Feng, R., Graf, T., 2004. Stepwise reprogramming of B cells into macrophages. Cell 117, 663–676.
Zhan, J., Deng, R., Tang, J., Zhang, B., Tang, Y., Wang, J.K., Li, F., Anderson, V.M., McNutt, M.A., Gu, J., 2006. The spleen as a target in severe acute respiratory syndrome. FASEB J. 20, 2321–2328.
Zukerberg, L.R., Collins, A.B., Ferry, J.A., Harris, N.L., 1991. Coexpression of CD15 and CD20 by Reed–Sternberg cells in Hodgkin's disease. Am. J. Pathol. 139, 475–483.